ISSN 0389-4010
UDC 621.454.2:
629.76

TECHNICAL REPORT OF NATIONAL AEROSPACE LABORATORY

TR-848T

Effective Specific Impulse of Secondary Flow Injected into a Rocket Nozzle

Hiroshi MIYAJIMA, Kazuo KUSAKA, and Eiji SOGAME

December 1984

NATIONAL AEROSPACE LABORATORY

CHŌFU, TOKYO, JAPAN

Effective Specific Impulse of Secondary Flow Injected into a Rocket Nozzle*

Hiroshi MIYAJIMA,** Kazuo KUSAKA,**
and Eiji SOGAME***

ABSTRACT

The effective specific impulse of secondary flow injected into a supersonic portion of a large-area ratio nozzle was evaluated experimentally. An oxygen/hydrogen thrust chamber with a 4000N thrust level and a chamber pressure of 3.5MPa was used. The secondary flow (ambient temperature hydrogen as a simulant of the oxygen/hydrogen turbine exhaust gas mixture) was injected through 30 discrete holes at a 13 : 1 local area ratio into a nozzle with a 140 : 1 overall area ratio. The mass flow ratio of secondary flow to primary flow was varied from 1 to 5%. Using a simple theory, experimentally obtained effective secondary flow specific impulse Is was compared with calculated results. The experimental Is value was consistently higher than the calculated value by about 20%, presumably because of mixing and heat transfer effects which were not taken into account in the theoretical calculation. The secondary flow film cooling effect was substantial and persisted up to the nozzle exit.

概　　要

大きな開口面積比のロケットノズル内へ送入した二次流の有効比推力を実験的に求めた。推力4KN，燃焼室圧力3.5MPaの水素／酸素ロケット推力室を用い，出口開口面積比140：1のノズルにおいて，開口比13：1の位置で，30個の横長の噴出口から常温の水素ガスを送入した。二次流の主流に対する質量流量比1～5%の範囲で実験をおこなった。推力測定による二次流の有効比推力の測定の他に，ノズル静圧，ならびに壁面への熱流束の分布におよぼす二次流の効果も実験した。簡単な理論による二次流の有効比推力の計算値と実験値の比較をおこなった。二次流量が主流の2%以上では実験値は計算値よりも約20%高かった。二次流によるフィルム冷却の効果は大きく，ノズル出口にまでおよんだ。

NOMENCLATURE

A^* : aerodynamic throat area
AR : local area ratio of primary nozzle
c^* : characteristic velocity
C_F : vacuum thrust coefficient
$C_F\,(th, \epsilon)$: theoretical one dimensional equilibrium vacuum thrust coefficient with area ratio ϵ
g : gravitational acceleration
I : vacuum specific impulse
$\dot{m}$: mass flow rate
MR_p : primary flow mixture ratio, oxygen to hydrogen mass flow rate ratio

* Received 26 November, 1984
** Kakuda Branch
*** National Space Development Agency of Japan

P_e : nozzle exit wall static pressure
P_O : stagnation pressure
P_{SM} : secondary manifold pressure
P_W : wall static pressure
$\dot{q}$: wall heat flux
R : gas constant
T_H : hydrogen supply temperature
γ : specific heat ratio
ϵ : overall nozzle area ratio
ϵ' : primary area ratio reduced by the secondary flow
η_{CF} : vacuum thrust coefficient efficiency
θ_e : primary nozzle exit angle

Subscript
E : engine, combined primary and secondary
p : primary flow
s : secondary flow
o : without secondary flow

1. INTRODUCTION

In many early gas generator cycle engine configurations the gases which drove the turbopumps were exhausted near the exit of main nozzle through a separate duct. However, by injecting turbine exhaust into the supersonic portion of the main nozzle, compact and lightweight engine packaging becomes possible. It also facilitates a wider angle of gimbaling. Moreover, if the engine is to be used for an upper stage of a launch vehicle, that process conveniently solves the separate localized secondary flow diffuser design problem for altitude firing test facility.

The secondary flow affects the delivered engine specific impulse. The secondary flow interacts with the primary flow, and the "effective" secondary flow specific impulse accounts for the decrease of primary flow specific impulse due to the addition of the secondary flow. The convention of effective specific impulse is particularly useful when multiple secondary streams contribute to the engine thrust, rendering separate evaluation of the specific impulses of primary and secondary flows possible. Numerous studies on secondary injection have been done in relation to film cooling.[1] A finite difference method developed by Beckwith and Bushnell[2] has been shown to provide generally accurate predictions for supersonic tangential slot injection. An accurate prediction of the expansion process of the secondary flow injected through discrete holes into the supersonic portion of a rocket nozzle is more difficult because primary and secondary flows interact in a complex manner. However, since the secondary flow rate is usually much smaller than the primary mass flow rate in a rocket engine, a simple method of analysis seems to be adoptable. Stromsta and Hosack[3] have developed such a simple method of analysis.

In the present study we measured the effective specific impulse of the secondary flow by using a low thrust oxygen/hydrogen thrust chamber with a large area ratio nozzle. The tests were conducted to simulate the effects of turbine exhaust on engine specific impulse of a 103 KN thrust oxygen/hydrogen engine, the LE-5, which will power the second stage of the next Japanese launch vehicle. The hardware used was approximately 1/5 scale. Measured effective specific impulses were compared with predicted impulses by the simple method of analysis noted above. Also, the measured film cooling effect of the secondary flow is briefly described.

2. TEST HARDWARE AND PROCEDURE

Figure 1 shows the thrust chamber assembly used for the turbine exhaust simulation test: a water cooled oxygen/hydrogen thrust chamber with a nominal thrust of 3950N at a chamber pressure of 3.4MPa. The mixture ratio of the primary flow was set at 5.5. The overall primary nozzle area ratio was 140:1. The nominal operating conditions and performance parameters of the primary flow are shown in Table 1, along

with the primary and secondary flow parameters which are required for the calculation of the secondary flow specific impulse. The secondary flow was injected through 30 discrete holes at a primary area ratio of 13:1, as shown in Fig. 1. The nozzle extension consisted of three segments with a total of 12 circumferential coolant passages to facilitate measurement of semilocal heat fluxes. The inner wall of the first segment was made of copper (OFHC), while that of the other segments was made of stainless steel.

The test article did not represent an exact

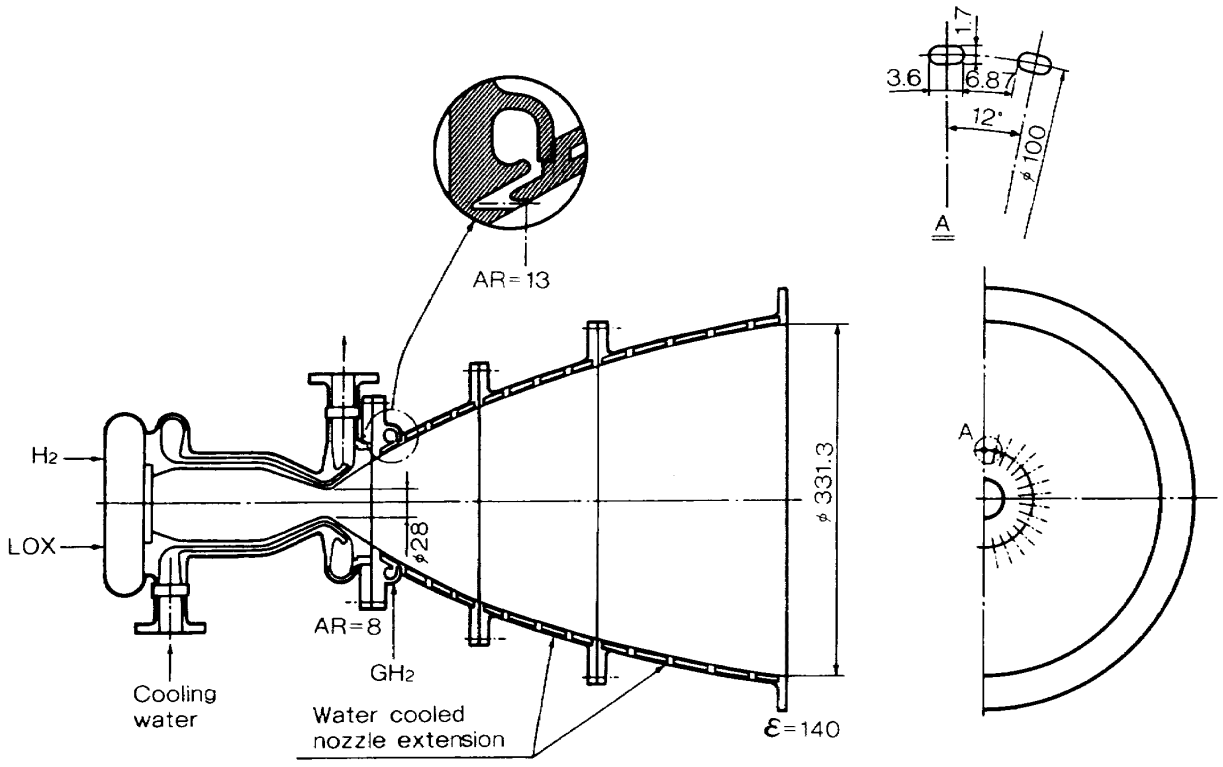

Fig. 1 Thrust chamber assembly

Table 1 Nominal operating conditions

Item	Mark	Unit	T_{HP} = 140K	T_{HP} = 290K
Chamber pr. (inj)	P_{op}	MPa	3.48	
Mixture ratio	MR	–	5.5	
Throat diameter	D_t	mm	28	
Primary nozzle area ratio	ϵ_p	–	140	
Injection area ratio	AR_i	–	13	
Nozzle exit angle	θ_e	deg	10.7	
Thrust	F	N	3964	3941
Charac. velocity	C^*	m/s	2245	2315
C^*-efficiency	η_{c^*}	–	.955	.975
Nozzle exit pr. ratio	Pe/P_{op}	–	$7.099*10^{-4}$	$7.296*10^{-4}$
Sec. hydrogen temp.	T_{HS}	K	280	290
Sec. charac. velocity	C_S^*	m/s	1516	1543
CFV efficiency	η_{CFP}	–	.959	.947
Theo. thrust coefficient	C_{FP} (th, ϵ_p)	–	1.997	2.004
Primary vac. I_{sp}	Ip/g	s	438	448

1/5 scale model of the LE-5 because of the incorporation of hardware from previous programs and the difficulty of fabricating the injection slits. In the full scale engine, 50 discrete slits are on the base of a back step at a primary nozzle area ratio of 8.5:1, the geometry of the injection step being formed by cutting a step off the otherwise smooth optimum thrust contour. In spite of these geometrical differences, it was considered that meaningful data could be obtained by hot firing tests.

Ambient temperature hydrogen was selected as a simulant of turbine exhaust gases in an oxygen/hydrogen engine. To estimate order of magnitude, the expansion process of the secondary flow was assumed to be the same as that in an equivalent Laval nozzle. The vacuum specific impulse is expressed as a product of characteristic velocity and vacuum thrust coefficient. For one dimensional flow of a perfect gas,

$$c_S^* = c_S^* (R_S, T_{OS}, \gamma_S) \quad (1)$$

$$C_{FS} = C_{FS} (\gamma_S, P_e/P_{OS}) \quad (2)$$

Since we are interested in the specific impulse, it is evident from Eqs. (1) and (2) that a good simulant should have the same characteristic velocity and specific heat ratio as that of the turbine exhaust (if the expansion pressure ratio are the same). The latter is determined from the primary area ratio and the secondary injection throat area. The primary area ratio was identical and the minimum secondary injection area was scaled proportionately in the present hardware. The pertinent physical parameters between the turbine exhaust and the simulant hydrogen are compared in Table 2. In view of its common availability, ambient temperature hydrogen is a satisfactory simulant.

All the experiments were conducted at the National Aerospace Laboratory's high altitude test facility for rocket engines. The capsule pressure was about 1KPa (8 torr). Initially, the specific impulses for various secondary flow injection rates were measured and then the effective secondary flow specific impulse was evaluated by comparison with the data for a smooth nozzle without secondary injection.[4] Estimated precision of the engine specific impulse was approximately 1%, most of the error being attributable to the measurement of hydrogen and oxygen mass flow rates. The secondary specific impulses obtained in this way scattered widely, especially for small secondary flow rates due to run-to-run reproducibilities of the performances. To eliminate this error, the secondary flow was injected during the initial 18 seconds and it was shut off in the remaining 4 to 8 seconds of a firing duration. Four seconds were sufficient for vacuum thrust decrement measurements. The division of this decrement by the secondary mass flow rate measured separately from the primary flow gave the effective secondary flow specific impulse.

Approximately 8 seconds were required to re-establish steady wall heat flux after the secondary flow was shut off. Since the secondary injection section is not cooled during the off time (see Fig. 1), repeated firing with 8 seconds off led to slight and gradual shrinkages of the

Table 2 Properties of turbine exhaust and simulant

	Mark	Unit	LE-5TE	Simulant H_2
Gas constant	R_S	J/kgK	2229	3849
Sec. temp.	T_S	K	650	300
Spc. heat ratio	γ_S	–	1.38	1.4
Charac. velo.	C_S^*	m/s	1767	1569

inner dimension of the upsteam end of the first segment of the nozzle extension, which led, in turn, to the termination of the test cycle.

3. SIMPLE THEORY

Even with current sophisticated numerical methods, it does not seem to be a simple matter to predict a detailed flow field of discrete secondary flow injection into a supersonic nozzle because of the three dimensional turbulent mixing, shock interactions, and separation and reattachment. However, since the secondary mass flow rate is usually much smaller than that of the primary flow, a simplified method of prediction can be used, as long as it gives a reasonable estimate of the effective secondary flow specific impulse.

Storomsta and Hosack[3] have developed such a simple method of analysis. The theory will be outlined here, since it is useful to subsequent discussion of the data. The flow model employed for the analysis is shown in Fig. 2. It is assumed that the introduction of secondary flow into the nozzle partially displaces the primary stream. To simplify the problem, the following assumptions are made:

1) No mixing between primary and secondary streams.
2) The secondary stream does not affect the primary nozzle efficiency.
3) Nozzle exit wall static pressure is not affected by the secondary flow.

With these assumptions, the ratio of vacuum specific impulse with secondary flow I_E to that without secondary flow I_p is expressed by

$$I_E/I_p = \frac{C_{Fp}(th, \epsilon'_p)}{C_{Fp}(th, \epsilon_p)} \frac{1 + \dfrac{\dot{m}_s c_s^* \eta_{CFs} C_{Fs}(th)}{\dot{m}_p c_p^* \eta_{CFp} C_{Fp}(th, \epsilon'_p)}}{1 + \dot{m}_s/\dot{m}_p} \tag{3}$$

c_s^* may be calculated from Eq. (1) and c_p^* can be determined from the experiment. Primay thrust coefficient efficiency η_{CFp} may be calculated by a detailed primary nozzle analysis. A standard method[6] is used for the calculation of theoretical one dimensional equilibrium thrust coefficient with a given area ratio. The remaining unknown parameters are η_{CFs}, $C_{Fs}(th)$ and ϵ'_p. The secondary thrust coefficient inefficiency is primarily caused by divergence effect. Thus,

$$\eta_{CFs} = \cos \theta_e \tag{4}$$

The secondary stream expansion area ratio ϵ_s and theoretical secondary thrust coefficient can be calculated from the isentropic relation,

$$\epsilon_s = A_e/A_s^* = \epsilon_s(\gamma_s, P_e/P_{Os}) \tag{5}$$

$$C_{FS}(th) = C_{FS}(th)(\gamma_s, \epsilon_s, P_e/P_{Os}) \tag{6}$$

Primary nozzle exit wall static pressure P_e may be obtained from a detailed nozzle analysis procedure. And, finally, the reduced area ratio of the primary stream is,

$$\epsilon'_p = (A_e - \epsilon_s A_s^*)/A_p^* \tag{7}$$

Once the ratio of vacuum specific impulses are calculated from Eq. (3), the effective secondary specific impulse I_s can be obtained from the following relationship.

$$I_E = (\dot{m}_p I_p + \dot{m}_s I_s)/(\dot{m}_p + \dot{m}_s) \tag{8}$$

It is noted from Eq. (8) that the primary specific impulse I_p is independent from the secondary stream, i.e., all decrements of the actual primary flow specific impulse are accounted for in the effective secondary flow specific impulse I_s.

The difficulty of applying the above analysis to practical problems lies in the determination of

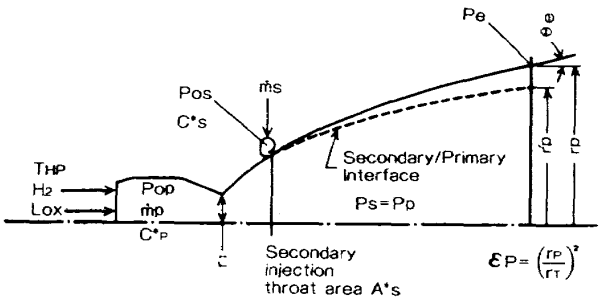

Fig. 2 Flow model for turbine exhaust I_{sp}

aerodynamic secondary throat area and secondary stagnation pressure, since isentropic relations are used in Eqs. (5) and (6). However, in view of the radically simplified nature of the analysis, P_{OS} was approximated by the measured secondary flow manifold pressure and A_S^* by the geometrical minimum area multiplied by the experimentally determined discharge coefficient.

4. EXPERIMENTAL RESULTS

4.1 Secondary Throat Area

As shown in Fig. 1, the minimum area of the secondary flow passage before injection is the cross sectional area of the injection hole. If the flow chokes in this minimum area, the secondary mass flow rate should be related to the secondary manifold pressure P_{SM} as a straight line through the origin. Fig. 3 shows good linearity except for a few data points near the secondary mass flow rate of 10g/s. In the lowest flow rate tested, it is suspected that a greater stream area reduction occured. However, since the deviation was very small, a constant value 0.773 was determined as the discharge coefficient. The aerodynamic secondary throat area was approximated by the geometrical minimum area multiplied by the discharge coefficient.

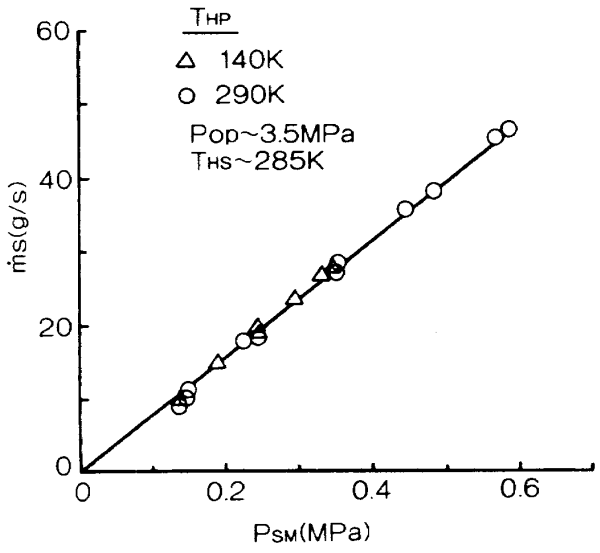

Fig. 3 Secondary flow rate vs. manifold pressure

4.2 Nozzle Exit Static Pressure

In the theory outlined above it was assumed that the secondary flow did not affect the primary nozzle exit wall static pressure. Let us examine this assumption.

Figure 4 shows the nozzle wall static pressure ratio as a function of primary nozzle area ratio for a secondary to primary mass flow ratio of approximately 1%. The static pressure ratio is expressed as (P_W/P_{OP}) with secondary flow to that without secondary flow $(P_W/P_{OP})_O$. The

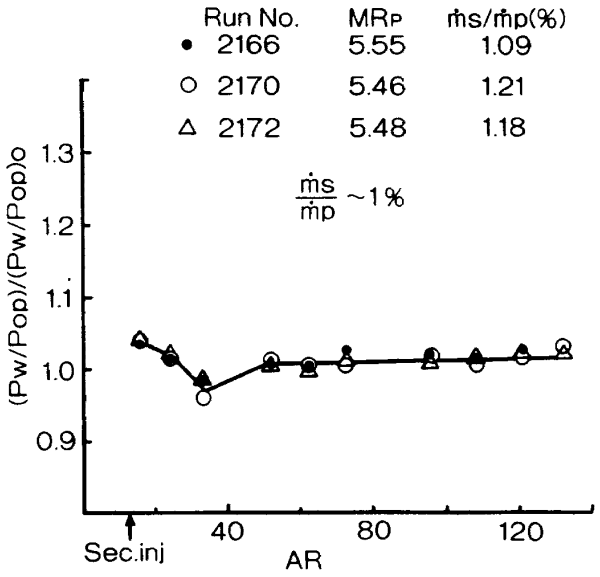

Fig. 4 Nozzle wall static pressure ratio for a secondary flow ratio of 1%

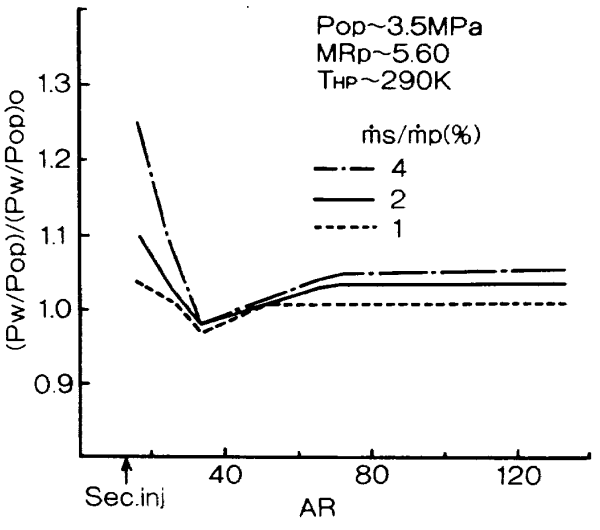

Fig. 5 Effect of secondary flow ratio on nozzle wall static pressure ratio

effect of the secondary flow rates on the pressure ratio is shown in Fig. 5. It is seen that the pressure ratio just downstream of the secondary injection was much greater than unity due to shock waves produced by the injection. The peak was higher for a greater secondary flow ratio. Downstream of the peak, the pressure ratio decreased to less than unity due to expansion waves, and then increased again until further large variations of the pressure ratio died down. For an area ratio greater than about 70, the pressure ratios attained constant values. The value was greater for a greater secondary flow ratio. For a 4 to 5% secondary flow ratio, the nozzle exit wall static pressure was higher by about 5% compared to that without secondary flow. The 5% increase in the nozzle exit wall static pressure corresponded to only a 0.12% decrease in the secondary thrust coefficient (Eqs. (5) and (6)). Thus the assumption that the secondary flow does not affect the primary nozzle exit wall static pressure seems to be a very good approximation for the present configuration and experimental conditions. The nozzle exit static pressure for zero-secondary flow may be calculated from a nozzle analysis code.[5] The effect of two dimensional flow should be taken into account for usual axisymmetric rocket nozzles.

4.3 Effective Secondary Specific Impuse

Figure 6 shows the experimental and calculated effects of secondary flow on the engine vacuum specific impulse and on the effective secondary flow vacuum specific impulse. The unit of secondary specific impulse is N-s/kg, but it was divided by gravitational acceleration for convenience. The theoretical curves correspond to the condition of primary hydrogen temperature of 290 K (Table 1). The calculated I_E/I_p and I_S for T_{Hp} = 140 K deviated from those for T_{Hp} = 290 K by about +0.025% and −1.2% respectively. It is also seen from the experimental data in Fig. 6 that the effect of primary hydrogen temperature was negligible.

The simple theory predicts the general trend of the effective secondary flow specific impulse for $\dot{m}_S/\dot{m}_p$ greater than 2%, although the magnitude of the predicted I_S was smaller than the experimental magnitude by about 20% (50 seconds). For a lower secondary mass flow ratio, i.e., $\dot{m}_S/\dot{m}_p < 2\%$, the experimental I_S increased with the decrease in the mass flow ratio, opposite to the trend predicted by the simple theory. This discrepancy between theoretical and experimental results is likely due to mixing and heat transfer between primary and secondary flows which was neglected in the simple theory. It should be noted that effects of shock and expansion waves are also neglected in the theory. However, since these aerodynamic effects generally reduce the primary specific impulse, which, in turn, reduces the effective secondary specific impulse, they are not likely the major factors for the discrepancy.

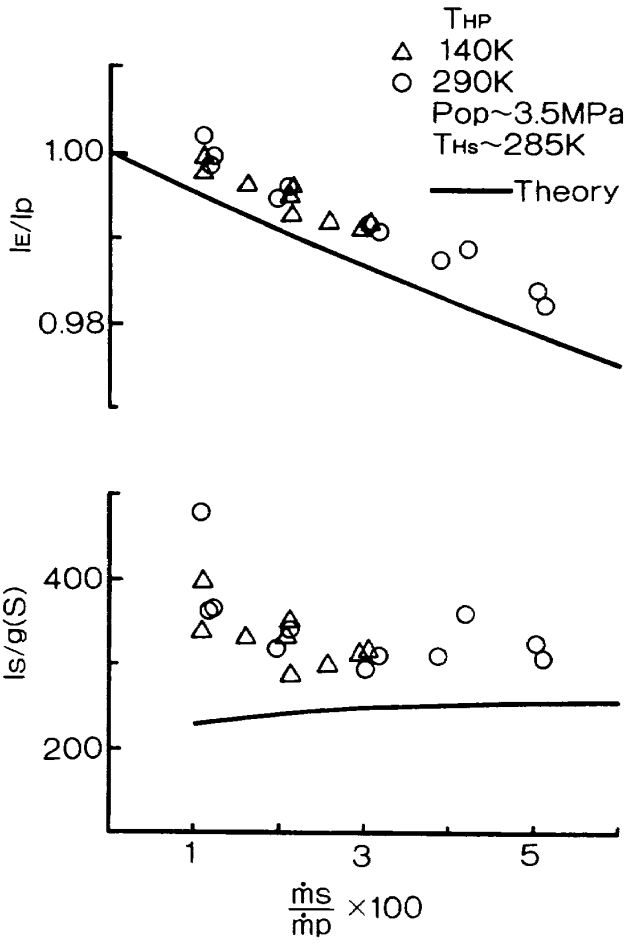

Fig. 6 Effective secondary flow specific impulse

Since a better, more convenient prediction method is not yet available, factors determined from the present experiment were used to analyse the performance of the full scale engine.[7] It is felt that a more realistic flow model is required to predict the effective secondary specific impulse more accurately.

4.4 Nozzle Heat Flux

When a secondary flow whose stagnation temperature is much lower than the primary recovery temperature is injected into a nozzle, heat flux to the nozzle wall decreases due to a film cooling effect. Figs. 7 and 8 show the heat flux with secondary flow to that without secondary flow as a function of primary nozzle area ratio. The heat fluxes were circumferentially averaged values, i.e., averaged over the wall covered and not covered by the gaseous film. Fig. 7 shows the degree of scatter of the measured heat flux. The effect of secondary flow ratio is summarized in Fig. 8. It is seen that the higher heat flux ratios were measured just downstream of the secondary injection, presumably due to the separation and reattachment of the primary flow. The behaviour of the heat flux ratio in this region is consistent with the pressure distribution shown in Figs. 4 and 5, i.e., the higher pressure ratio corresponds to a higher heat flux ratio. Downstream of the minimum heat flux ratio, the heat flux ratio gradually increased. The film cooling effect depended on the secondary mass flow ratio and persisted up to the nozzle exit.

It should be noted that the secondary flow was injected through 30 discrete holes rather than a circumferentially continuous slot. As shown in Fig. 1, only 34% of the periphery is covered by the injection holes. This could be a very inefficient configuration for cooling. However, from heat marks on the copper surface just downstream of the secondary injection (Fig. 9a), it may be seen that the secondary flow attached to the surface about 20 to 30 mm downstream of the injection holes, covering a much greater periphery of the wall. The above observation seems to be consistent with the heat flux data shown in Figs. 7 and 8, i.e., the minimum heat flux ratios approximately corresponds just downstream of the attached secondary flow. It is also seen from the streaks in Fig. 9b that the identity of each stream injected from each hole seems to be preserved down-

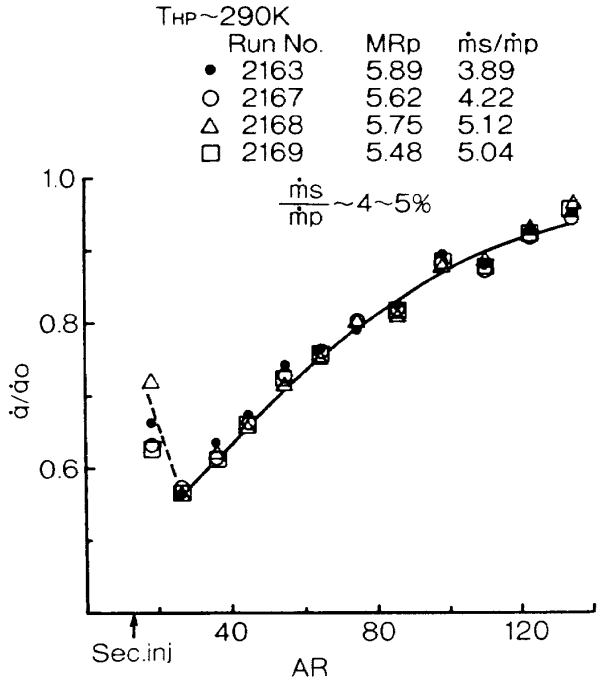

Fig. 7 Heat flux ratio for 4 to 5% secondary mass flow ratio

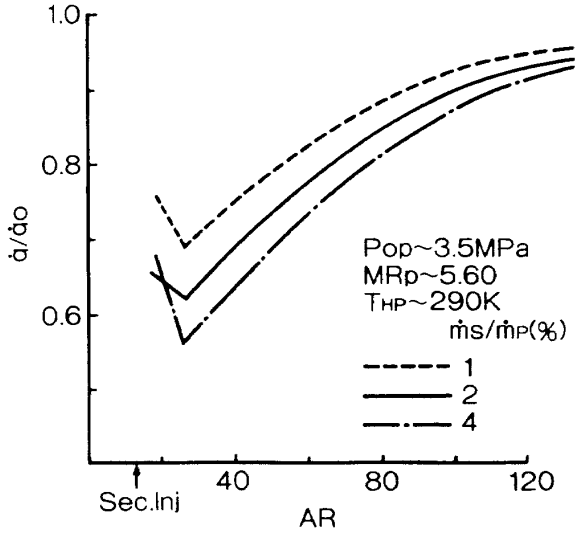

Fig. 8 Effect of secondary flow ratio on heat flux ratio

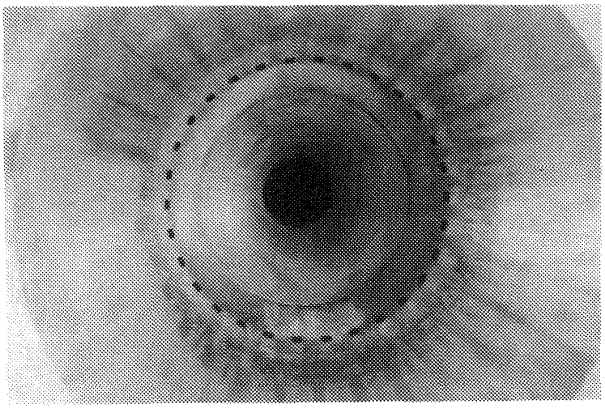

a

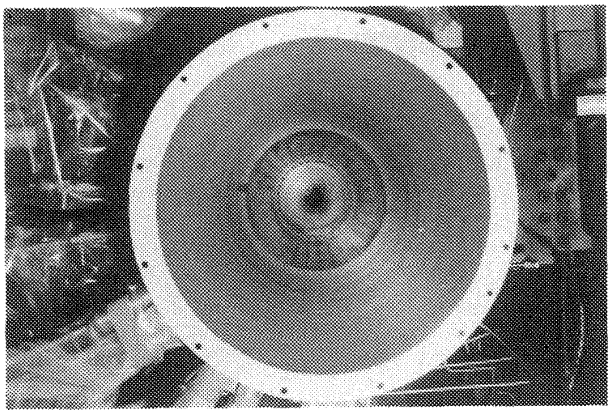

b

Fig. 9 Heat marks on nozzle wall

stream.

Since the coverage of the injection slits was about 76% of the periphery of the full scale engine, the cooling effect there is expected to be more efficient than that of the present experiment.

5. CONCLUDING REMARKS

Effective specific impulse of the secondary flow injected into a supersonic portion of a large area ratio nozzle was measured using a 4000N thrust level oxygen/hydrogen thrust chamber. The results are summarized as follows:

1) The experimental effective vacuum specific impulse of the secondary flow was about 20% greater than that calculated from the simple theory.
2) The nozzle exit wall static pressure with secondary flow was only slightly higher than that without secondary flow, verifying one of the assumptions of the simple theory.
3) The film cooling effect of the secondary flow was substantial and persisted up to the nozzle exit.

A more realistic flow model is required to improve the prediction accuracy of the secondary specific impulse, as well as to predict the film cooling effect. However, for a quick estimation of effective secondary flow specific impulses, the simple theory, combined with the factors determined from the present experiment, is useful.

REFERENCES

1) Goldstein, R.J., "Film Cooling", Advances in Heat Tranfer, Vol. 7, Accademic Press, New York, 1971, pp. 321-379.
2) Beckwith, I.E., and Bushnell, D.M., "Calculation by a Finite-Difference Method of Supersonic Turbulent Boundary Layers with Tangential Slot Injection", NASA TN D-6221, April 1971.
3) Stromsta, R.R., and Hosack, G.A., "Analytical Methods for Computing the Effects of Turbine Exhaust and Film-Coolant Injection on Rocket Engine Performance", AIAA paper 69-473, 1969.
4) Miyajima, H., et al., "Performance of a Small LO2/LH2 Thrust Chamber with High Area Ratio Nozzles", Proc. 13th Intn. Symposium on Space Tech. & Sci., Tokyo, 1982, pp. 253-258, AGNE Pub. Inc., Tokyo, 1982.
5) Nakahashi, K., Miyajima, H., Kisara, K., and Moro, A., "Prediction Method of Rocket Nozzle Performance", Technical Report of the National Aerospace Lab. NAL TR-771, July 1983.
6) Gordon, S. and McBride, B.J., "Computer Program for Calculation Complex Chemical Equilibrium Compositions, Rocket Perfomances, Incident and Reflected Shocks, and Chapman-Jouget Detonations", NASA SP-

237, 1971.

7) Miyajima, H., Nakahashi, K., Yanagawa, K., and Fujita, T., "Specific Impulse Analysis of the LE-5", AIAA paper 84-1224, June 1984.

TECHNICAL REPORT OF NATIONAL
AEROSPACE LABORATORY
TR-848T

航空宇宙技術研究所報告848T号(欧文)

昭和59年12月発行

発行所 航空宇宙技術研究所
東京都調布市深大寺東町7丁目44番地1
電話武蔵野三鷹(0422)47-5911(大代表)〒182
印刷所 株式会社 東京プレス
東京都板橋区桜川2－27－12

Published by
NATIONAL AEROSPACE LABORATORY
1,880 Jindaiji, Chōfu, Tokyo
JAPAN

Printed in Japan